

Mitigating Hallucinations in YOLO-based Object Detection Models: A Revisit to Out-of-Distribution Detection

Weicheng He^{1,*}, Changshun Wu^{1,*}, Chih-Hong Cheng^{2,3}, Xiaowei Huang⁴, and Saddek Bensalem⁵

Abstract—Object detection systems must reliably perceive objects of interest without being overly confident to ensure safe decision-making in dynamic environments. Filtering techniques based on out-of-distribution (OoD) detection are commonly added as an extra safeguard to filter hallucinations caused by overconfidence in novel objects. Nevertheless, evaluating YOLO-family detectors and their filters under existing OoD benchmarks often leads to unsatisfactory performance. This paper studies the underlying reasons for performance bottlenecks and proposes a methodology to improve performance fundamentally. Our first contribution is a calibration of all existing evaluation results: Although images in existing OoD benchmark datasets are claimed not to have objects within in-distribution (ID) classes (i.e., categories defined in the training dataset), around 13% of objects detected by the object detector are actually ID objects. Dually, the ID dataset containing OoD objects can also negatively impact the decision boundary of filters. These ultimately lead to a significantly imprecise performance estimation. Our second contribution is to consider the task of hallucination reduction as a joint pipeline of detectors and filters. By developing a methodology to carefully synthesize an OoD dataset that semantically resembles the objects to be detected, and using the crafted OoD dataset in the fine-tuning of YOLO detectors to suppress the objectness score, we achieve a 88% reduction in overall hallucination error with a combined fine-tuned detection and filtering system on the self-driving benchmark BDD-100K. Our code and dataset are available at: <https://gricad-gitlab.univ-grenoble-alpes.fr/dnn-safety/m-hood>.

I. INTRODUCTION

In image classification, research has shown (e.g. [1]) that deep neural network-based classifiers can be overly confident in their predictions. Since object detection involves both localization and classification, overconfidence also manifests itself. For dynamic driving tasks, it is crucial to eliminate the impact of overconfidence. Failure to do so can lead to unsafe scenarios, such as the unintended activation of automatic emergency braking due to falsely detected pedestrians.

Out-of-distribution (OoD) detection is one promising approach to mitigating the impact of overconfidence in new or unfamiliar situations. Within image classification, OoD detection techniques can filter anomalies and correct the result from the predicted class to the artificially introduced “OoD” class. Transferring the techniques from classification



(a) Test images used in VOS [2] that should be diagnosed as OoD accidentally contain ID “car” objects.



(b) ID images used in VOS [2] for shaping the decision boundary containing OoD objects such as penguins and camels.

Fig. 1: Quality issues in existing OoD evaluation benchmarks that lead to non-optimal performance

into object detection, techniques such as VOS [2], SAFE [3] and BAM [4] are implemented on top of Faster-RCNN [5] as an extra component to subsequently filter the detected and classified objects by setting these objects to be of class “OoD”. A recent study [6] migrates state-of-the-art OoD detection methods in classification to YOLO series of object detectors. Despite the superior performance of OoD detectors operated on Faster-RCNN, the performance is still far from acceptable and reveals a significant improvement potential in YOLO.

In this paper, we analyze the reasons behind the unsatisfactory OoD detection performance and design a methodology to improve the overall performance of mitigating hallucination errors (i.e., false detections) when encountering OoD samples. Our first result is identifying *dataset quality issues and benchmark design* in evaluating OoD used in VOS [2] and all other techniques, contributing to the high false positive rates observed in previous studies. Specifically, we uncover two critical problems and *study their impact both in theory and concrete empirical evaluations*:

- Existing OoD test datasets have many “OoD” classified images. However, these images contain objects holding in-distribution (ID) classes, i.e., categories defined in the object detector training dataset. Consider the example

*Equal contribution, ordered alphabetically by last name.

¹ Université Grenoble Alpes, Grenoble, France.

² Chalmers University of Technology, Gothenburg, Sweden.

³ University of Gothenburg, Gothenburg, Sweden.

⁴ University of Liverpool, Liverpool, UK.

⁵ CSX-AI, Grenoble, France.

Correspondence to: changshun.wu@univ-grenoble-alpes.fr

in Fig. 1a where an image is considered as “OoD”, any prediction of a “car” object in that image will be counted as a hallucination error. Due to the dataset design and the evaluation pipeline, an image’s “OoD” labeling is only on the *whole image level* (i.e., not on the bounding box level). Such a labeling creates an *implicit assumption* that an “OoD” image should not contain any ID object. However, as shown in later sections, around 13% of objects detected in “OoD” images are actually ID. This implies that the performance for prior results is higher than the reported numbers by removing dataset errors.

- For constructing the decision boundary of filters, existing frameworks use *FPR95* (false positive rate at 95% true positive rate) as a guiding principle. The decision boundary threshold is adjusted so that 95% of the distribution samples are correctly classified. The ID images used to calibrate decisions also contain potentially diagnosed OoD objects counted as errors (see Fig. 1b for examples), so the intended decision boundary can be influenced, leading to worse performance.

To further reduce the hallucination (overconfident predictions) caused by OoD samples, we introduce a novel approach to forge a defensive decision boundary against OoD samples via fine-tuning. Unlike classification models, object detectors are inherently trained to differentiate foreground objects from background objects, often using the *objectness score*. As OoD filtering is only triggered when the object detector acknowledges the existence of an object, reducing the false detection can be done as a *joint approach*: In addition to equipping a filter similar to that of VOS or BAM, additionally adjust the decision boundary of the object detector to reduce opportunities to trigger false detections. Specifically, we introduce a fine-tuning strategy that uses a set of OoD samples proximal to ID data - termed “proximal OoD” - which can be inferred from the ID data distribution without relying on specific test-time OoD datasets. From the perspective of learned “concepts”, these samples share high-level semantic features with ID data while differing in low-level attributes, effectively bridging the gap between ID and truly novel OoD instances. During fine-tuning of the models on these proximal OoD samples, the model is trained to treat proximal OoD samples as background, thereby shaping an implicit defensive decision boundary against general OoD instances. Our experimental results show that this method effectively mitigates hallucinations when encountering both near-OoD and far-OoD inputs, demonstrating its efficacy.

In summary, our main contributions are as follows:

- We identify key dataset quality issues in existing OoD benchmarks that negatively impact the evaluation of OoD detection methods in YOLO models.
- We propose a novel fine-tuning approach that leverages objectness properties to construct a more robust defensive decision boundary against OoD samples.
- We conduct extensive experiments that demonstrate the effectiveness of our approach, achieving substantial

improvements in both near-OoD and far-OoD detection scenarios.

II. RELATED WORK

Overconfidence or hallucination is a symptom that can arise in both ID and OoD scenarios, where our work focuses on the OoD case. OoD detection has gained significant attention in computer vision. Within image classification tasks, techniques leveraging confidence scores [7], [8], [9], feature-space distances [10], [11], [12], [13] or generative modeling [14], [15] can detect OoD anomalies. We refer readers to a recent survey paper [16] for a detailed summary of techniques. Due to the maturity of OoD detection research in classification, the community has developed a standard benchmark OpenOoD [17], enabling researchers to compare against different techniques. For OoD detection in object detection, the problem is less explored despite its importance, and as of the time of writing (March 2025), OpenOoD has not yet supported object detection. Methods operated on Faster-RCNN, including VOS [2], SAFE [3] and BAM [4] enable reducing hallucination in OoD samples via refining feature space representations and uncertainty estimation. The recent study [6] translated multiple OoD detection methods within classification to the YOLO-family object detection settings, including maximum logits (MLS) [18], maximum softmax probability (MSP) [19], energy-Based methods (EBO) [8], Mahalanobis distance (MDS) [10], k-nearest neighbors (KNN) [12] and the recent SCALE method [9]. While the performance of reducing hallucination against OoD samples has been considerably superior to those applied on Faster-RCNN, it is still far from satisfactory. Our result in highlighting problems within the existing object detection OoD benchmark dataset implies that the performance of prior results should be better than the reported numbers. It also stresses the importance of having a rigorous benchmark to ensure an unbiased performance evaluation. Furthermore, our proposed fine-tuning based on introducing proximal OoD examples in the detector is experimentally proven to be highly effective. It also reflects the design principle that reducing hallucination when encountering novel or abnormal objects should be a joint effort (similar to adversarial training [20] for adversarial robustness) between the object detector and the subsequent filter that performs OoD detection.

III. OOD PROBLEM AND BENCHMARK ANALYSIS

Existing Benchmark. Existing benchmarks for evaluating OoD detection in object detection, including those by existing results [3], [4], [6] continue to utilize the datasets introduced in the work of VOS [2]. These benchmarks claim that the OoD test datasets do not contain any object that overlaps with one of the ID classes. However, we have identified critical issues within these datasets that contribute to inflated FPR95 values, ultimately undermining the accuracy of the evaluation. In the following, we formulate the observed phenomenon and analyze these issues in detail.

A. Issues in Benchmark Datasets - Theoretical Analysis

Let f be an object detector that takes an image I and produces a set $f(I) \stackrel{\text{def}}{=} \{(b_i, y_i)\}$ of bounding box (b_i) and the associated label (y_i). The label y_i is within the list of ID object classes \mathcal{O}_{in} . In the example of applying f under the KITTI dataset [21], \mathcal{O}_{in} includes classes such as car, van, or truck. For OoD detection, it is achieved by furthering applying a *filtering function* $g(b_i, I)$ to each predicted object b_i in image I , where g outputs a score that reflects the confidence of the object not within the ID classes. A threshold τ is then applied to the score such that if $g(b_i, I) < \tau$, the object is classified as ID, and the label y_i is kept the same. Otherwise, it is classified as OoD and y_i is updated to a special class `ood`, i.e., $y_i \leftarrow \text{ood}$ where `ood` $\notin \mathcal{O}_{\text{in}}$.

1) *How OoD-only test sets are evaluated:* Given an image I , let $G_{\mathcal{O}_{\text{in}}}(I) \stackrel{\text{def}}{=} \{(\hat{b}_i, \hat{y}_i)\}$ be the associated ground truth object label associated with \mathcal{O}_{in} . An *OoD-only test set* $\mathcal{D}_{\text{test}}^{\text{OoD}}$ contains only images I where $G_{\mathcal{O}_{\text{in}}}(I) = \emptyset$, i.e., there exists no object \hat{b}_i whose true class \hat{y}_i is within \mathcal{O}_{in} . To evaluate the performance of the detector f and the OoD filter g against $\mathcal{D}_{\text{test}}^{\text{OoD}}$, one iteratively takes $I \in \mathcal{D}_{\text{test}}^{\text{OoD}}$, generate predictions and apply filtering. As $G_{\mathcal{O}_{\text{in}}}(I) = \emptyset$, the number of hallucinations made in f combined with g can be summarized using Eq. (1). It is the number of generated bounding boxes whose labels are not changed to `ood`.

$$err_{f,g}^+(I) \stackrel{\text{def}}{=} |\{(b_i, y_i) \mid (b_i, y_i) \in f(I), g(b_i, I) < \tau\}|$$

provided that $I \in \mathcal{D}_{\text{test}}^{\text{OoD}}$ (1)

2) *Type-1 data error: ID Objects in OoD Test Sets:* We can now describe the Type 1 data error and its associated consequences. A Type 1 error occurs when an image in the OoD-only test set contains at least one ID object (i.e., belonging to \mathcal{O}_{in}). An example of this issue is shown in Fig. 1a. Precisely, an *OoD-only test set* $\mathcal{D}_{\text{test}}^{\text{OoD}}$ manifests **Type 1 data errors** iff the following holds:

$$\exists I \in \mathcal{D}_{\text{test}}^{\text{OoD}} \text{ such that } G_{\mathcal{O}_{\text{in}}}(I) \neq \emptyset \quad (2)$$

Consequently, if f is very successful in detecting objects specified in \mathcal{O}_{in} , the impact of data error will be more likely to be reflected in the evaluation to be counted as the false positive made by f and g .

Lemma 1: Given $I \in \mathcal{D}_{\text{test}}^{\text{OoD}}$ where $G_{\mathcal{O}_{\text{in}}}(I) \neq \emptyset$, and assume that f detects a bounding box with success probability α . The expected value of false positives (hallucinated objects) made by f and g , caused by the Type 1 data error, equals $\alpha|G_{\mathcal{O}_{\text{in}}}(I)|$.

Proof: The lemma holds as every ID-object in $G_{\mathcal{O}_{\text{in}}}(I)$ within an OoD-only image can be detected by f with a probability of α .

3) *How ID-only data set is used for deciding FPR95 decision boundary for the OoD filter:* To set the threshold τ for deciding whether an object shall be considered as OoD or ID, the criterion of FPR95 (false positive rate at 95% true

positive rate) is used. This means that τ is adjusted on the ID-only dataset $\mathcal{D}_{\text{cali}}^{\text{ID}}$ where the OoD filter achieves a 95% success rate in “not to consider an object as OoD”. Counting the errors made in an image within $\mathcal{D}_{\text{cali}}^{\text{ID}}$ is based on Eq. (3). We use an example to assist in understanding Eq. (3): If there is a car in the image where the object detector successfully detects it (i.e., $(b_i, y_i) \in f(I)$), but the OoD filter negatively considers it an OoD object (i.e., $g(b_i, I) \geq \tau$), it should be counted as an error of g .

$$err_{f,g}^-(I) \stackrel{\text{def}}{=} |\{(b_i, y_i) \mid (b_i, y_i) \in f(I), g(b_i, I) \geq \tau\}|$$

provided that $I \in \mathcal{D}_{\text{cali}}^{\text{ID}}$ (3)

Based on the FPR95 principle, one then carefully adjusts the threshold τ such that within $\mathcal{D}_{\text{cali}}^{\text{ID}}$, total error rate $err_{\mathcal{D}_{\text{cali}}^{\text{ID}}}$ remains less than 5%, where $err_{\mathcal{D}_{\text{cali}}^{\text{ID}}}$ is defined using Eq. (4).

$$err_{\mathcal{D}_{\text{cali}}^{\text{ID}}} \stackrel{\text{def}}{=} \frac{\sum_{I \in \mathcal{D}_{\text{cali}}^{\text{ID}}} err_{f,g}^-(I)}{\sum_{I \in \mathcal{D}_{\text{cali}}^{\text{ID}}} |\{(b_i, y_i) \mid (b_i, y_i) \in f(I)\}|} \quad (4)$$

4) *Type 2 data issue: Unlabelled OoD Objects in ID-only data sets:* Unfortunately, the above experiment design is based on an assumption where *there exist no OoD objects* that an object detector f can be wrongly triggered. Precisely, an *ID-only dataset* $\mathcal{D}_{\text{cali}}^{\text{ID}}$ manifests **Type 2 data issues** iff the following holds, where \hat{y}_i is the associated ground truth:

$$\exists I \in \mathcal{D}_{\text{cali}}^{\text{ID}} \text{ such that } \exists (b_i, y_i) \in f(I) : \hat{y}_i = \text{ood} \quad (5)$$

Consider the images illustrated in Fig. 1b, where they belong to $\mathcal{D}_{\text{cali}}^{\text{ID}}$. Consider if an object detector f wrongly detects the camel as an object within class \mathcal{O}_{in} , and the filter g successfully filters it. Then, the condition in Eq. (3) holds, so it will be counted as an error made by the OoD filter g .

In the following, we explain the impact on the decision boundary τ to be integrated into the OoD filter g by considering one construction method L_2 -norm-based OoD filter. Techniques such as BAM or Mahalanobis distance share the same characteristic, so the proof strategy can be easily adapted to other OoD filters.

Given an object detector f with input $I \in \mathcal{D}_{\text{cali}}^{\text{ID}}$, let $f^{-l}(b_i, I)$ be the feature vector at layer l that generates bounding box b_i . Let c be the arithmetic mean of all feature vectors for all boxes in $\mathcal{D}_{\text{cali}}^{\text{ID}}$, i.e.,

$$c \stackrel{\text{def}}{=} \frac{\sum_{I \in \mathcal{D}_{\text{cali}}^{\text{ID}}} \sum_{(b_i, y_i) \in f(I)} f^{-l}(b_i, I)}{\sum_{I \in \mathcal{D}_{\text{cali}}^{\text{ID}}} \sum_{(b_i, y_i) \in f(I)} 1} \quad (6)$$

Consider an OoD filter $g(b_i, I) \stackrel{\text{def}}{=} \|f^{-l}(b_i, I), c\|_2$ that computes the L_2 norm between the feature vector and the center c . Therefore, τ is defined based on the distance from the feature vector to the center (mean). Consider using FPR95 to decide τ , where the construction is illustrated using Fig. 2. One sorts the feature vectors by distances (to center) from large to small. Subsequently, start by setting τ to be the largest distance τ_{max} , and greedily introduce a

feature vector with the next smaller distance τ' and update τ to τ' . When adjusting τ , ensure that $err_{\mathcal{D}_{\text{cal}}^{\text{ID}}}$ remains to be below 5%. Let τ_1 in Fig. 2 be the radius where the currently computed error rate is exactly 5%. We discuss the impact of including $f^{-l}(b_i, I)$ in the design of τ , where b_i contains an OoD object (triggering Type 2 data issue).

- Based on the standard evaluation pipeline, then shrinking τ from τ_1 to $g(b_i, I)$ makes the condition $g(b_i, I) \geq \tau$ in Eq. (3) from false to true, implying that the resulting error rate $err_{\mathcal{D}_{\text{cal}}^{\text{ID}}}$ (with small radius) will be increased, thereby being larger than 5%.
- If one changes the evaluation pipeline where bounding box b_i can be evaluated against the ground-truth label “ood”, the prediction over b_i will be counted as correct. Consequently, shrinking τ from τ_1 to $g(b_i, I)$ still keeps $err_{\mathcal{D}_{\text{cal}}^{\text{ID}}}$ to be $\leq 5\%$.

Therefore, having an image with a bounding box containing an OoD object in the ID dataset (without labeling these objects as “ood” and enabling an evaluation pipeline) increases the length of τ . As a larger τ implies weaker capabilities in filtering OoD objects (recall in Fig. 2, where everything inside the circle is counted as ID by filter g), the capability of distance-based OoD filters, when there exist unlabeled OoD objects within the ID dataset, can be compensated.

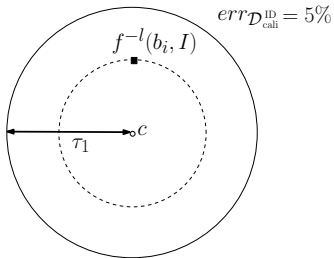


Fig. 2: Understanding the impact of decision boundary when unlabeled OoD object occurs in an ID-only dataset

The following summarizes our theoretical analysis; in the subsequent sections, we provide a quantitative analysis of the concrete benchmark suites supporting our findings.

- Fixing Type 1 data issues requires carefully removing ID objects within an OoD-only dataset.
- Fixing Type 2 data issues requires labeling all potentially identified OoD objects in bounding boxes (to let an OoD detector’s response be counted as correct) within an ID-only dataset.¹

B. Issues in Benchmark Datasets - Quantitative Analysis

We quantitatively analyze Type 1 error in the widely used OoD test dataset, OpenImages [22], designed for evaluating OoD detection methods for two ID tasks: PASCAL-VOC [23] and BDD-100K [24]. For brevity, we refer to this subset as OpenImages throughout this paper. We focus on instances where ID objects are erroneously included in the

¹Alternatively, design a pipeline that every object outside the labelled ones is automatically counted as OoD.

benchmark OoD-only test set, potentially distorting evaluation metrics. We leverage a high-accuracy pre-trained object detection model trained on OpenImagesV7 [22], which recognizes over 500 categories. By running inference on the entire OpenImages dataset, we systematically identify images containing ID objects that should not have been classified as OoD. Our analysis reveals that among the 1,852 images in the dataset, 104 images (5.62%) contain at least one ID object despite being labeled as OoD. Across these images, we detect 220 ID objects, accounting for 12.75% and 13.77% of all detected objects by the models for PASCAL-VOC and BDD-100K tasks (see Table I). To measure the impact of these mislabeling errors on OoD detection performance, we evaluate FPR95 with and without the erroneously labeled images. Our results in Table I show that Type 1 error inflates FPR95 by 9.85% and 5.58% in PASCAL-VOC and BDD-100K tasks, respectively, demonstrating a significant distortion in evaluation metrics. These findings underscore the need for more rigorous dataset curation to ensure the reliability of OoD detection benchmarks.

TABLE I: Quantitative analysis of type 1 error: Estimation of the prevalence of ID object in OoD test set and its impact on OoD detection evaluation.

ID Dataset	OoD Dataset	Prevalence	FPR95 Inflation
PASCAL-VOC	OpenImages	12.75%	+9.85%
BDD-100k	OpenImages	13.77%	+5.58%

Given the large number of predictions—nearly 200,000 in BDD-100K and nearly 20,000 in PASCAL-VOC—it is impractical to assign each prediction an accurate ID/OoD label. Therefore, for the Type 2 issue, we approximately quantify its impact on evaluation through a pre-trained model by estimating the number of OoD objects present in the ID test sets of the PASCAL-VOC and BDD-100K tasks. As shown in Table II, 16.52% of images in the BDD-100K dataset and 8.69% in the PASCAL-VOC dataset contain at least one OoD object, which is non-negligible.

TABLE II: Quantitative analysis of Type 2 issues: Estimation of ID and OoD object counts in the BDD-100K and PASCAL-VOC datasets using a pre-trained model.

ID Dataset	Type	Objects	Samples (%)
BDD-100K	ID	185,945	10,000
	OoD	8,129	1,652 (16.52%)
PASCAL-VOC	ID	12,648	4,952
	OoD	746	430 (8.69%)

C. ID Outlier-induced Ambiguity

Apart from Type 1 and Type 2 data issues, we identify another potential reason why OoD detection methods struggle in YOLO models: the existence of “ID outlier objects” (i.e., visually atypical ID objects in some particular ID categories) within the ID test dataset. For instance, Fig. 3 shows “ID outlier objects” in the “Bird” category of PASCAL-VOC, including visually atypical birds. Our experiments reveal

that these ID outlier objects often receive exceptionally high OoD scores—sometimes even higher than most actual OoD samples. As shown in Fig. 4, the presence of ID outliers increases the threshold τ required to retain 95% of ID detections (analogous to the result in Sec. III-A.4). As a result, under this inflated OoD score threshold, many OoD samples are incorrectly classified as ID objects, meaning the OoD detector fails to filter them out effectively, leading to a high FPR95 value.



Fig. 3: Visualization of ID outliers in the “Bird” category in PASCAL-VOC: atypical bird samples with rare shapes or colors that deviate from the main category distribution.

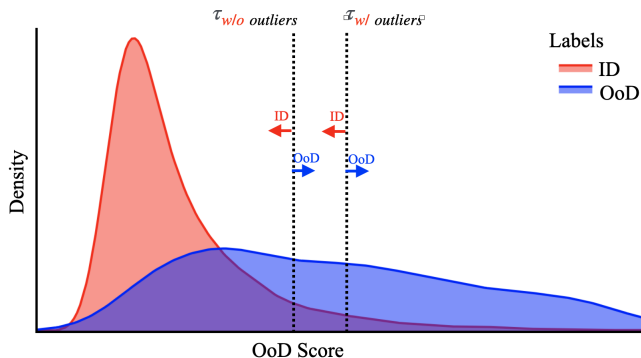


Fig. 4: Kernel Density Estimation (KDE) plot of the OoD scores for a KNN-based OoD filter, on a benchmark where the ID task is PASCAL-VOC and the OoD test dataset is OpenImages. A higher score indicates a higher likelihood of being an OoD object. The thresholds $\tau_{w/o \text{ outliers}}$ and $\tau_{w/ \text{ outliers}}$ are chosen to ensure a 95% recall for ID detections. The presence of outliers shifts the threshold, leading to more OoD samples being misclassified as ID samples, thereby reducing the effectiveness of OoD detection.

Considering the presence of these outliers, we advocate evaluating OoD filter methods on both the original dataset and a version with outliers removed. For instance, in Table III, we present a comparison showing that OoD filter methods perform significantly better without these outliers. To filter outliers, we employ a distance-based identification technique [12] that uses box plots to detect potential outliers within each category.

D. New Benchmarks

As discussed in previous sections, existing OoD benchmark datasets are prone to dual mislabeling errors, limiting their reliability for OoD evaluation. We introduce two

TABLE III: Comparison of OoD filters, with and without outliers, on a benchmark where the ID task is PASCAL-VOC, and the OoD test dataset is OpenImages. In the absence of outliers, these filters perform better, as reflected in lower FPR95 scores.

Condition	MSP	EBO	MLS	MDS	SCALE	BAM	KNN
w/ outliers	0.7164	0.9307	0.9220	0.8457	0.6803	0.5306	0.5376
w/o outliers	0.6797	0.9301	0.9208	0.8410	0.6296	0.4479	0.4467

new OoD benchmark datasets, Near-OoD and Far-OoD², designed based on image semantics and empirical difficulty to address this issue. Near-OoD includes objects semantically similar to training categories, often presenting empirical challenges for the model due to their resemblance to ID classes. At the same time, Far-OoD consists of more semantically distant objects, including background images without recognizable objects. Each dataset consists of approximately 1,000 images sourced from the OpenImagesV7 dataset, covering over 500 diverse object detection categories. To ensure the integrity of these benchmarks, we verify that none of the images contain objects from the training categories. This is initially done by performing inference with a pre-trained, high-accuracy YOLO model on OpenImagesV7. We then analyze the model’s predictions and filter out images containing indisputable objects from training categories. Finally, a manual inspection is conducted for further validation.

IV. FINE-TUNING FOR MITIGATING HALLUCINATION

This section introduces an alternative strategy to mitigate YOLO’s hallucination (overly confident predictions) on OoD samples without explicitly performing OoD detection. Our approach leverages proximal OoD samples, which are semantically similar to the ID categories but do not belong to them. This fine-tuning method, similar to adversarial training, adjusts the model’s decision boundaries to make it more conservative when facing OoD samples. This reduces the likelihood of hallucinated predictions, whereas adversarial training focuses on enhancing the model’s robustness against adversarial examples. Rather than training a model from scratch, we adopt a fine-tuning strategy that is computationally efficient and effective in reshaping the decision boundary. By guiding the model to differentiate between proximal OoD data and ID samples, we hypothesize that it can better generalize and distinguish broader OoD instances. We first describe the construction of the proximal OoD dataset and then introduce our fine-tuning methodology.

A. Proximal OoD Dataset Construction

A well-curated proximal OoD dataset is essential for fine-tuning the model effectively to mitigate hallucinations caused by OoD samples. We first establish selection principles for identifying suitable samples to construct such a dataset.

²<https://gricad-gitlab.univ-grenoble-alpes.fr/dnn-safety/m-hood>

- *Non-overlapping with training categories:* Selected samples must not belong to any training categories to prevent unintentional inclusion of ID samples.
- *Conceptual or visual similarity:* Chosen samples should be related to or visually resemble training categories, allowing the model to learn meaningful variations.
- *Proxy category reuse:* Similar training categories may share common proxy categories when applicable. For instance, “cat” and “dog” can have overlapping proxy categories due to their similar visual characteristics.

To construct a high-quality proximal OoD dataset, we leverage Caltech 256 [25], a diverse object-centric dataset, as a source of candidate samples. Given the large number of categories, manual selection is impractical. Instead, we employ a reasoning-based large language model (LLM) to generate candidate categories that align with our selection principles, followed by manual verification to ensure their validity. Fig. 5 presents the prompt template used to generate candidate proximal OoD categories. Once the proximal OoD categories are identified, we collect approximately 2,000 images and ensure they do not contain any ID objects, as they will serve as background or negative samples during fine-tuning. We systematically analyze the dataset using a pre-trained vision model to enforce this constraint. The model automatically filters out images containing training categories. This automated refinement minimizes ID contamination while preserving the diversity of OoD samples. Finally, the curated dataset is converted into the YOLO format, ensuring seamless integration into the fine-tuning pipeline. This approach streamlines dataset construction and enhances the reliability of proximal OoD selection, enabling more effective mitigation of overconfident predictions.

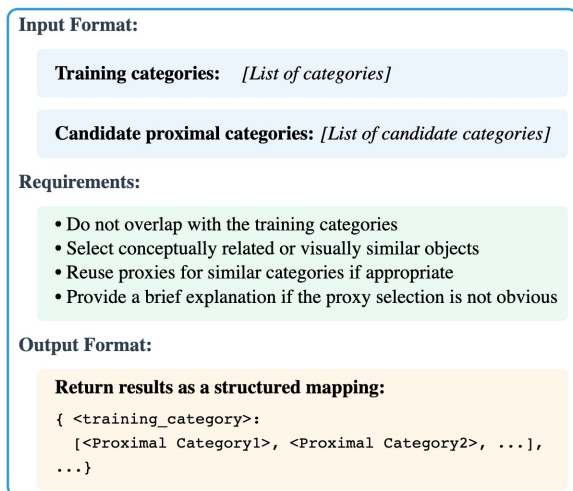


Fig. 5: Prompt template for generating candidate proximal OoD categories.

B. Fine-Tuning Strategy

To mitigate hallucinated predictions while preserving detection performance, we fine-tune the model using a dataset comprising both the original ID training set \mathcal{D}_{train} and the

proximal OoD sample set \mathcal{D}_{prox} constructed in the previous subsection. The only modification during training is treating proximal OoD samples as background, preventing the model from assigning high confidence scores. The classification loss for ID samples remains as in YOLOv10 [26], while for proximal OoD samples, all detected objects are treated as negatives (background). The total classification loss is defined as:

$$\mathcal{L}_{cls}^{ft} = \mathcal{L}_{cls}^{\mathcal{D}_{train}} + \lambda \mathcal{L}_{cls}^{\mathcal{D}_{prox}} \quad (7)$$

Where λ controls the influence of proximal OoD data, this adjustment reduces hallucinations while maintaining detection accuracy.

V. EXPERIMENTS

This section details the experimental setup, evaluates the fine-tuned model’s performance, and presents empirical results demonstrating the effectiveness of our fine-tuning method in reducing hallucinations caused by OoD samples.

A. Experimental Setup

We evaluate our method on two well-trained YOLOv10 models from [26], trained on PASCAL-VOC and BDD-100K, respectively. We use the calibrated near-OoD and far-OoD datasets introduced in the previous subsection to assess hallucinations. The effectiveness of fine-tuning is measured by its ability to reduce hallucinations, which we quantify using OoD counts—the number of predictions on OoD data. Ideally, this value should be zero. However, ensuring that the model’s primary detection performance is not compromised beyond mitigating hallucinations is crucial. To this end, we track mean average precision (mAP) to evaluate the model’s accuracy on ID data.

B. Fine-tuning

We fine-tune the YOLOv10 models for 20 epochs on a combined dataset of their training data and proximal OoD samples collected in the previous section, following the default training configuration of YOLOv10 in [26]. Specifically, we use the Stochastic Gradient Descent (SGD) optimizer with a momentum of 0.937 and a weight decay of 5×10^{-4} . The initial learning rate is set to 0.01 and decays linearly to 0.0001 throughout the fine-tuning process. Training is performed on a single NVIDIA V100 GPU with a batch size of 64.

During fine-tuning, we observe the mAP on the ID validation set to analyze model performance change. At the same time, we evaluate the model hallucinations by measuring the number of predictions on OoD data. Fig. 6 illustrate mAP changes over epochs and the trend in hallucination counts on OoD datasets during fine-tuning for the ID task of BDD-100K. The results show that mAP initially declines before gradually improving and returning to its original value by the end of the 20 epochs. This is likely due to the inclusion of proximal OoD data, which presents the model with more challenging backgrounds (similar to ID categories). As it adapts, ID performance temporarily declines. Over

time, the model adapts by refining its decision boundaries, regaining ID performance while learning to handle the more challenging OoD data.

Meanwhile, hallucination on both OoD datasets drop sharply in the first epoch and stabilize at a lower level after several epochs (around 20% of the original), suggesting that the model becomes more conservative early in fine-tuning, reducing overconfident predictions. We selected a version for further analysis, reducing OoD detections by up to 80% with only a 1% decrease in ID performance. This version strikes a balance between ID task accuracy and hallucination suppression.

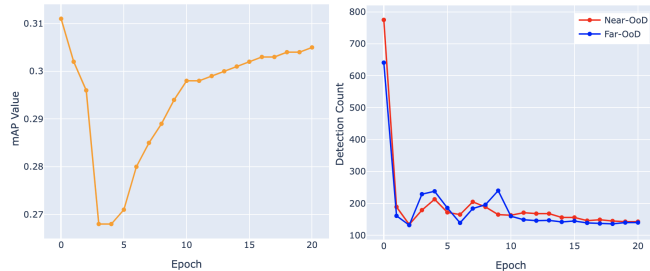


Fig. 6: Fine-tuning trends of YOLOv10 model pre-trained on BDD-100K: mAP evolution (left), and prediction counts on OoD datasets (right).

C. Effectiveness Evaluation

In this subsection, we evaluate the effectiveness of our fine-tuning approach in mitigating hallucinations in YOLO models when exposed to OoD samples. Our analysis consists of two key aspects: (1) the impact of fine-tuning alone and (2) the additional benefits of integrating an OoD detector with the fine-tuned model.

Impact of Fine-Tuning To quantify the reduction in hallucinations, we compare the number of OoD detections before and after fine-tuning across different datasets, as shown in Table IV. Fine-tuning leads to a substantial decrease in mis-detections across both ID tasks. For example, in the BDD-100K dataset, the number of detected Near-OoD samples drops from 708 to 145, and a similar reduction is observed in other settings. This trend highlights the effectiveness of fine-tuning in suppressing spurious detections on OoD data. A qualitative comparison is provided in Fig. 7, where the fine-tuned model demonstrates fewer hallucinated predictions (highlighted in red bounding boxes) than the original model. This visual evidence further supports the ability of our fine-tuning approach to mitigate hallucinated predictions.

TABLE IV: OoD counts comparison of different models.

ID Dataset	OoD Datasets	Original	Original+ KNN	Fine-tuned	Fine-tuned+ KNN
BDD-100K	Near-OoD	708	297	145	78
	Far-OoD	641	290	136	83
PASCAL-VOC	Near-OoD	991	424	364	195
	Far-OoD	431	176	140	87

Integrating an OoD Detector To further mitigate hallucinations, we integrate an OoD detector into the fine-tuned model. Our evaluation consists of two steps: first, we assess the performance of various OoD detection methods, and second, we analyze the combined effect of fine-tuning and the best-performing detector. Table V presents the results of our OoD detector evaluation, where BAM and KNN consistently outperform other baselines. Notably, KNN achieves slightly better performance than BAM. Given its superior performance, we use KNN combined with the original and fine-tuned models to examine their respective contributions to reducing hallucinations. Table IV shows that fine-tuning alone significantly improves model reliability, reducing hallucination counts across all datasets. Notably, in the BDD-100K task, the fine-tuned model without an OoD detector significantly reduced hallucinations, with the number of Near-OoD predictions dropping from 297 (Original + BAM) to 145 and Far-OoD predictions decreasing from 290 to 136. When KNN is combined with the fine-tuned model, hallucination counts are further reduced by over 40%, demonstrating the additional benefit of leveraging an OoD detector. Specifically, as shown in Table IV, on the BDD-100K benchmark, this combination results in a near 88% reduction in hallucination counts compared to the original model. The original model generated 708 and 641 hallucinations on the near- and far-OoD datasets, respectively, which reduced to 78 and 83 after applying our method. Similarly, for the PASCAL-VOC task, hallucinations decrease by 80.3%.

VI. CONCLUSION AND FUTURE WORK

This work examined the challenges of OoD detection in YOLO-based object detectors, identifying key dataset quality issues that contribute to high false positive rates. We found that mislabeling in OoD test datasets and anomalies within ID datasets significantly affect evaluation outcomes, underscoring the need for improved benchmarks. Additionally, we proposed a novel approach to reducing model sensitivity to OoD samples: a fine-tuning strategy that leverages the objectness property of YOLO models. Our method effectively establishes a defensive decision boundary by training on proximal OoD samples, significantly reducing hallucinations caused by OoD samples in YOLO models. Future work includes developing quantifiable, hierarchical OoD definitions to generalize proximal OoD samples into hierarchical ones, enabling a more precise characterization of the forged defensive decision boundary. Another aspect of future work will focus on selecting OoD data sources, including real and synthetic data.

REFERENCES

- [1] D. Hendrycks and K. Gimpel, "A baseline for detecting misclassified and out-of-distribution examples in neural networks," in *ICLR*, 2017.
- [2] X. Du, Z. Wang, M. Cai, and S. Li, "Towards unknown-aware learning with virtual outlier synthesis," in *ICLR*, 2022.
- [3] S. Wilson, T. Fischer, F. Dayoub, D. Miller, and N. Sünderhauf, "Safe: Sensitivity-aware features for out-of-distribution object detection," in *ICCV*, pp. 23565–23576, 2023.

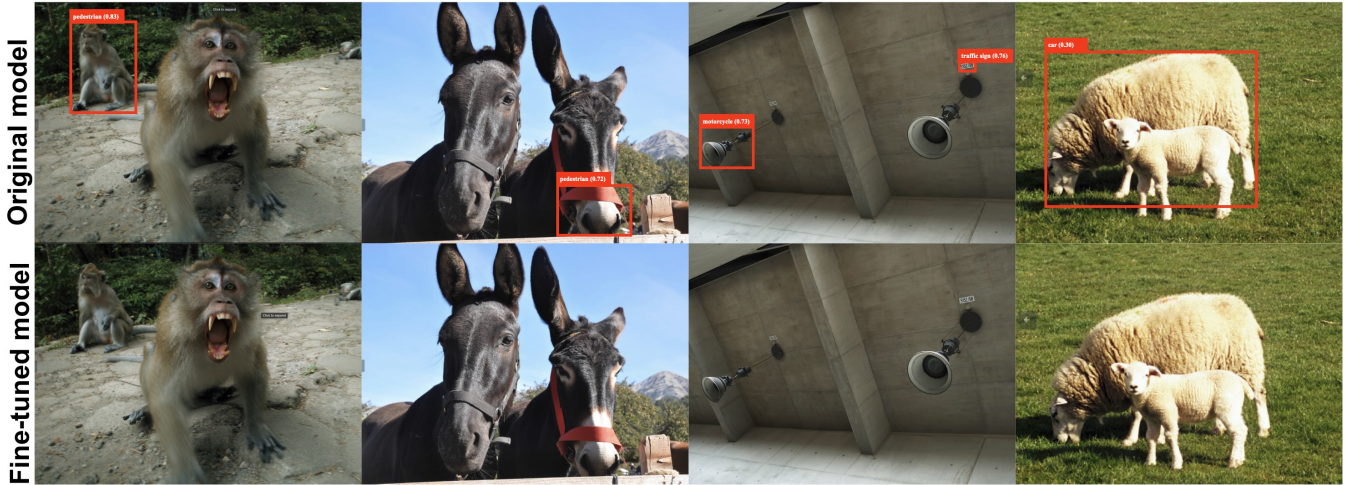


Fig. 7: Qualitative comparison of predictions on OoD images using the original and fine-tuned models. (Top) The original model produces hallucinated predictions. (Bottom) The fine-tuned model mitigates hallucinations, enhancing safety in decision-making.

TABLE V: Comparison of OoD filter performance on fine-tuned models using FPR95.

ID Dataset	OoD Dataset	Condition	MSP [19]	EBO [8]	MLS [18]	MDS [10]	SCALE [9]	BAM [4]	KNN [12]
PASCAL-VOC	Near-OoD	w/ outliers	0.7879	0.9174	0.9036	0.7080	0.8154	0.6006	0.6061
		w/o outliers	0.7713	0.9174	0.9036	0.6694	0.8099	0.5207	0.5344
	Far-OoD	w/ outliers	0.7214	0.8786	0.8571	0.7500	0.7500	0.6714	0.6857
		w/o outliers	0.7071	0.8857	0.8571	0.7143	0.7286	0.6357	0.6214
BDD-100K	Near-OoD	w/ outliers	0.8333	0.9028	0.8819	0.6944	0.8194	0.6944	0.5972
		w/o outliers	0.7917	0.9028	0.8819	0.6528	0.8056	0.6667	0.5417
	Far-OoD	w/ outliers	0.8162	0.9118	0.8897	0.8529	0.7721	0.7941	0.6985
		w/o outliers	0.7941	0.9118	0.8897	0.8382	0.7721	0.7426	0.6103

- [4] C. Wu, W. He, C.-H. Cheng, X. Huang, and S. Bensalem, "BAM: box abstraction monitors for real-time ood detection in object detection," in *IROS*, pp. 2632–2638, IEEE, 2024.
- [5] S. Ren, K. He, R. Girshick, and J. Sun, "Faster R-CNN: Towards real-time object detection with region proposal networks," *NeurIPS*, vol. 28, 2015.
- [6] W. He, C. Wu, and S. Bensalem, "Box-based monitor approach for out-of-distribution detection in YOLO: An exploratory study," in *RV*, pp. 229–239, Springer, 2024.
- [7] S. Liang, Y. Li, and R. Srikant, "Enhancing the reliability of out-of-distribution image detection in neural networks," in *ICLR*, 2018.
- [8] W. Liu, X. Wang, J. Owens, and Y. Li, "Energy-based out-of-distribution detection," *NeurIPS*, vol. 33, pp. 21464–21475, 2020.
- [9] K. Xu, R. Chen, G. Franchi, and A. Yao, "Scaling for training time and post-hoc out-of-distribution detection enhancement," in *ICLR*, 2024.
- [10] K. Lee, K. Lee, H. Lee, and J. Shin, "A simple unified framework for detecting out-of-distribution samples and adversarial attacks," *NeurIPS*, vol. 31, 2018.
- [11] C.-H. Cheng, G. Nührenberg, and H. Yasuoka, "Runtime monitoring neuron activation patterns," in *DATE*, pp. 300–303, IEEE, 2019.
- [12] Y. Sun, Y. Ming, X. Zhu, and Y. Li, "Out-of-distribution detection with deep nearest neighbors," in *ICML*, pp. 20827–20840, PMLR, 2022.
- [13] C. Wu, Y. Falcone, and S. Bensalem, "Customizable reference runtime monitoring of neural networks using resolution boxes," in *RV*, pp. 23–41, Springer, 2023.
- [14] J. Ren, P. J. Liu, E. Fertig, J. Snoek, R. Poplin, M. Depristo, J. Dillon, and B. Lakshminarayanan, "Likelihood ratios for out-of-distribution detection," *NeurIPS*, vol. 32, 2019.
- [15] H. Kamkari, B. L. Ross, J. C. Cresswell, A. L. Caterini, R. Krishnan, and G. Loaiza-Ganem, "A geometric explanation of the likelihood ood detection paradox," in *ICML*, pp. 22908–22935, PMLR, 2024.
- [16] J. Yang, K. Zhou, Y. Li, and Z. Liu, "Generalized out-of-distribution detection: A survey," *IJCV*, vol. 132, no. 12, pp. 5635–5662, 2024.
- [17] J. Yang, P. Wang, D. Zou, Z. Zhou, K. Ding, W. Peng, H. Wang, G. Chen, B. Li, Y. Sun, *et al.*, "Openood: Benchmarking generalized out-of-distribution detection," *NeurIPS*, vol. 35, pp. 32598–32611, 2022.
- [18] D. Hendrycks, S. Basart, M. Mazeika, A. Zou, J. Kwon, M. Mostajabi, J. Steinhardt, and D. Song, "Scaling out-of-distribution detection for real-world settings," in *ICML*, pp. 8759–8773, PMLR, 2022.
- [19] D. Hendrycks and K. Gimpel, "A baseline for detecting misclassified and out-of-distribution examples in neural networks," in *ICLR*, 2017.
- [20] F. Tramer and D. Boneh, "Adversarial training and robustness for multiple perturbations," *NeurIPS*, vol. 32, 2019.
- [21] A. Geiger, P. Lenz, and R. Urtasun, "Are we ready for autonomous driving? the kitti vision benchmark suite," in *CVPR*, pp. 3354–3361, IEEE, 2012.
- [22] A. Kuznetsova, H. Rom, N. Alldrin, J. Uijlings, I. Krasin, J. Pont-Tuset, S. Kamali, S. Popov, M. Mallocci, A. Kolesnikov, T. Duerig, and V. Ferrari, "The open images dataset v4: Unified image classification, object detection, and visual relationship detection at scale," *IJCV*, 2020.
- [23] M. Everingham, L. Van Gool, C. K. Williams, J. Winn, and A. Zisserman, "The pascal visual object classes (voc) challenge," *IJCV*, vol. 88, pp. 303–338, 2010.
- [24] F. Yu, H. Chen, X. Wang, W. Xian, Y. Chen, F. Liu, V. Madhavan, and T. Darrell, "Bdd100k: A diverse driving dataset for heterogeneous multitask learning," in *CVPR*, pp. 2636–2645, 2020.
- [25] G. Griffin, A. Holub, and P. Perona, "Caltech 256," Apr 2022.
- [26] A. Wang, H. Chen, L. Liu, K. Chen, Z. Lin, J. Han, *et al.*, "Yolov10: Real-time end-to-end object detection," *NeurIPS*, vol. 37, pp. 107984–108011, 2025.